

Article

Wavelet Packet-Fuzzy Optimization Control Strategy of Hybrid Energy Storage Considering Charge–Discharge Time Sequence

Xinyu Zhao ¹, Yunxiao Zhang ¹, Xueying Cui ¹, Le Wan ¹, Jinlong Qiu ¹, Erfa Shang ², Yongchang Zhang ¹ and Haisen Zhao ^{1,*} 

¹ College of Electrical and Electronic Engineering, North China Electric Power University, Beijing 102206, China; 120212201327@ncepu.edu.cn (X.Z.); 120212201089@ncepu.edu.cn (Y.Z.); 120202201339@ncepu.edu.cn (X.C.); 120222201757@ncepu.edu.cn (L.W.); 120222201388@ncepu.edu.cn (J.Q.); zyc@ncepu.edu.cn (Y.Z.)

² Inner Mongolia Xilin Gol League Dian Tou New Energy Co., Ltd., Xilinhot 026000, China; seftl@sina.com

* Correspondence: zhaohisen@ncepu.edu.cn

Abstract: A hybrid energy storage system (HESS) can effectively suppress the high and low-frequency power fluctuations generated by wind farms under the intermittency and randomness of wind. However, for the existing power distribution strategies of HESS, power-type and energy-type energy storage have the problem of inconsistent charge–discharge states in the same time sequence, which makes it difficult to achieve optimal operation in terms of charge–discharge coordination and energy flow. To solve this problem, this study firstly adopts adaptive wavelet packet decomposition (WPD) to decompose the original wind power to acquire grid-connected power and HESS initial distribution power, to ensure that the supercapacitor and battery undertake the corresponding high and low-frequency power fluctuations, respectively; Then, for the inconsistent charge–discharge states, a charge–discharge time sequence optimization strategy based on the consistency index is proposed to correct the initial power distribution of HESS for the first time; Finally, aiming at the stage of charge (SOC) over-limit problem, the fuzzy optimization method is adopted to correct the HESS output power for the second time, which can reduce the unnecessary charge–discharge energy effectively. With typical daily output data of a 100 MW wind farm, the proposed control strategy is verified. The results show that it can make different energy storage technologies synchronously suppress wind power fluctuation in the same time sequence; compared with not considering charge–discharge time sequence optimization, the charge–discharge conversion times of the battery obtained by the proposed method are reduced from 71 to 14 times, and the charge–discharge conversion times of supercapacitor are reduced from 390 to 61 times; The cumulative reduction of unnecessary charge–discharge energy by HESS is 12.12 MWh. Besides, the SOC curves of HESS are controlled at a normal level, thus improving the economy and service life of HESS.

Keywords: hybrid energy storage system; wind power suppression; charge–discharge time sequence optimization; wavelet packet decomposition; fuzzy optimization



Citation: Zhao, X.; Zhang, Y.; Cui, X.; Wan, L.; Qiu, J.; Shang, E.; Zhang, Y.; Zhao, H. Wavelet Packet-Fuzzy Optimization Control Strategy of Hybrid Energy Storage Considering Charge–Discharge Time Sequence. *Sustainability* **2023**, *15*, 10412. <https://doi.org/10.3390/su151310412>

Academic Editors: Valeria Palomba and Thanikanti Sudhakar Babu

Received: 17 April 2023

Revised: 5 June 2023

Accepted: 29 June 2023

Published: 1 July 2023



Copyright: © 2023 by the authors. Licensee MDPI, Basel, Switzerland. This article is an open access article distributed under the terms and conditions of the Creative Commons Attribution (CC BY) license (<https://creativecommons.org/licenses/by/4.0/>).

1. Introduction

Wind power output is characterized by intermittent and volatility. The direct grid connection of wind power has a significant impact on the stability of the power system. How to effectively suppress the fluctuation of wind power and improve its grid-connected operation ability is of great practical importance for the utilization of wind power [1–4]. The existing energy storage technologies consist of two categories: energy-type and power-type, among which energy-type energy storage has high energy density, low power density and short cycling life, which is not applicable for a fast charge–discharge; Power-type energy storage has low energy density and high power density, frequent charge–discharge will not damage its performance. In view of the excellent performance complementarity of the two kinds of energy storage, many studies use them to form HESS to suppress wind power fluctuations [5–9].

Generally, hierarchical optimization of wind power suppression was carried out according to energy storage SOC in [10,11], which can realize wind power suppression and HESS normal operation through low-pass filtering, power regulation and limit management. A novel dynamic power-distribution control based on multi-filter was proposed for HESS integrated with a grid-connected wave energy converter [12], which can effectively suppress the output power before grid connection. The wind power suppression methods by HESS based on empirical mode decomposition (EMD) were proposed in [13–15]. A two-level real-time wavelet decomposition (WD) method was used to dispose of wind power [16]. The first-level filtering can obtain the power that meets the fluctuation demand; the second-level filtering can remove the noise produced by the rolling of the filtering window; Besides, the HESS can normally work through the SOC feedback control. In [17], WPD theory was used to dispose of the output fluctuation of wind power, the wind power is decomposed into low-frequency signal reflecting grid-connected power and the high-frequency signal connected to HESS, and then the high-frequency signal was further decomposed based on the properties of HESS. An evaluation index based on intermittent power supply fluctuation and micro-grid supply and demand balance was established, and a HESS charge–discharge method on the basis of WPD and fuzzy control were presented in [18], which can improve the fluctuation of intermittent power supply in micro-grid and reduce unbalanced power. Fuzzy logic control was used to control the energy management system with HESS priority order in [19,20], which can control SOC at a normal level.

At present, several studies put forward corresponding strategies of HESS to control its SOC at a normal level on the premise of suppressing wind power fluctuation. However, in the HESS power distribution strategies acquired by filtering, EMD, WPD and other methods, when wind power fluctuation is small, energy-type and power-type energy storage both get power instructions. Besides, there is a problem of inconsistent charge–discharge states of each energy storage in the same time sequence, which increases the charge–discharge conversion times, and makes HESS undertake extra energy absorption and release, resulting in the reduction of economy and service life.

To solve the above problems, firstly, adaptive WPD is adopted to decompose the original wind power to acquire grid-connected power and HESS initial distribution power so that the battery and supercapacitor can undertake the corresponding high and low-frequency power fluctuations, respectively. Then, for the inconsistent charge–discharge states, a charge–discharge time sequence optimization method based on the consistency index is proposed to correct the initial power distribution of HESS for the first time. Finally, aiming at the SOC over-limit problem, the fuzzy optimization method is adopted to correct the HESS power for the second time, and the unnecessary charge–discharge energy can be effectively reduced. With a 100 MW wind farm, the superiority of the proposed method is verified and analyzed from three aspects: suppression effect, charge–discharge time sequence optimization effect and SOC optimization effect. The validation results show that the adaptive WPD method has a good suppression effect on the original wind power fluctuation, and the grid-connected power that meets the fluctuation standard is obtained. The proposed charge–discharge time sequence optimization method can make different energy storage technologies synchronously charge or discharge in the same time sequence and effectively reduce the charge–discharge conversion times and accumulated charge–discharge energy. Besides, the fuzzy control method considering charge–discharge time sequence can reduce the charge–discharge depth of the energy storage system and prevent excessive charge–discharge, thus improving the economy and service life of HESS.

2. Wind Storage System Structure and Grid-Connected Power Acquisition

2.1. Wind Storage System Structure

Figure 1 shows the typical wind storage system structure; it includes wind farm, HESS, power grid and energy management system. Based on the comprehensive evaluation of the current market status of battery energy storage technology, lithium iron phosphate battery is regarded as one of the most competitive energy storage technologies in the future of large-

scale application due to its advantages of high specific power, high specific energy, long lifetime and continuous declining cost. Therefore, HESS is mainly composed of lithium iron phosphate batteries, supercapacitors, DC/DC converters and DC/AC inverters. The battery and the supercapacitor are connected to the DC bus through their respective DC/DC boost circuits, and then the DC power of HESS is converted into AC power through the DC/AC inverter circuit. Finally, the output power of the wind farm, battery and supercapacitor is collected into the common bus (PCC) and then flows to the power grid together. The energy management system can control the energy absorption and release of HESS reasonably by collecting the SOC and output of each device to suppress wind power fluctuation.

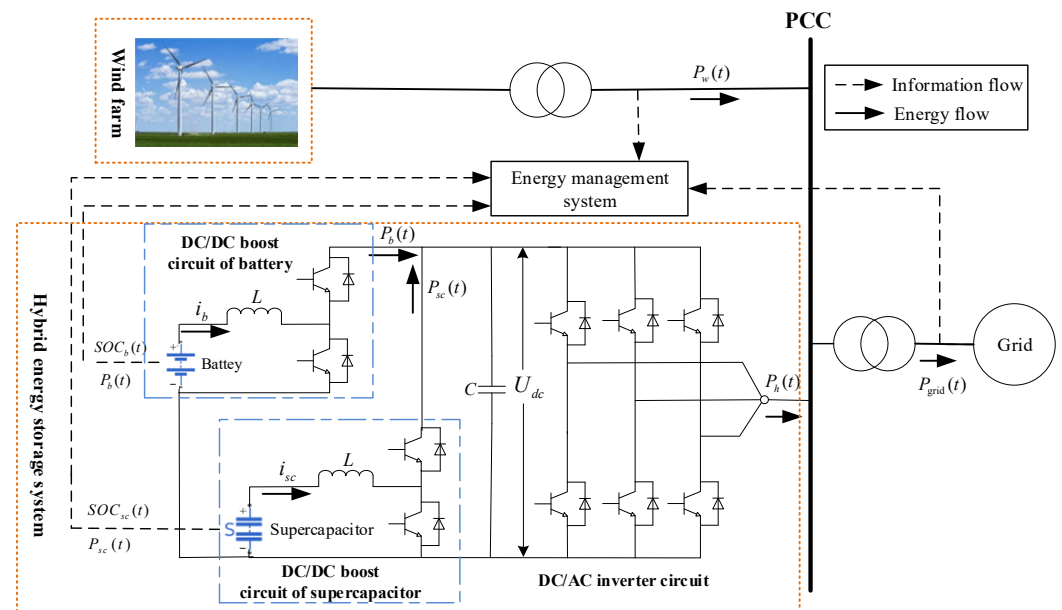


Figure 1. Wind storage system structure.

The energy flow relationship in the wind storage system is shown in (1) and (2).

$$P_{\text{grid}}(t) = P_w(t) + P_h(t) \quad (1)$$

$$P_h(t) = P_b(t) + P_{sc}(t) \quad (2)$$

where $P_{\text{grid}}(t)$, $P_w(t)$ are the output power of grid-connected point and wind farm, respectively; $P_h(t)$, $P_b(t)$, $P_{sc}(t)$ are the output power of HESS, battery and supercapacitor, respectively; $P_b(t) > 0$ or $P_{sc}(t) > 0$ represents that the battery or supercapacitor is discharging; On the contrary, $P_b(t) < 0$ or $P_{sc}(t) < 0$ represents that the battery or supercapacitor is charging. Units of all the above parameters are “MW” in this study.

2.2. Grid-Connected Power Acquisition of Wind Storage System Based on Adaptive WPD

With the purpose of decreasing the adverse effects of wind power fluctuation on the stability of power grid operation, many nations have established corresponding standards for grid connection of wind power, among which GB/T 19963-2011 in China stipulates the maximum limits of wind power variation at 1 min and 10 min time scales [21], as shown in Table 1.

In order to maximize the economic benefits of HESS and the utilization rate of wind power generation, it is only required to ensure that the wind power fluctuation meets the grid-connected standard in Table 1. Among filtering, EMD, WD, WPD, and other decomposition methods, traditional filtering decomposition is sensitive to the fluctuation characteristics of wind power, its general applicability is poor, and the filtering time constant is difficult to control accurately. EMD has the problems with boundary effect and mode

aliasing. WD has multiple resolution properties in processing unsteady mutation signals. On the premise of WD, WPD further improves the time-frequency resolution of signal analysis and helps to obtain the details of the high-frequency signal. Besides, the calculation speed of WD and WPD is faster than EMD. Since the signal studied in this study is based on the real-time fluctuation power data of wind farms, the variation of wind power is large and irregular under the condition of poor wind speed, so the decomposition method with outstanding signal mutation decomposition ability and time-frequency local analysis ability should be selected. Based on the above analysis, WPD is more applicable for the analysis of wind power properties. So WPD is adopted to decompose the fluctuating output power of wind farms. The basic principle of WPD is to represent the wavelet packet with an analysis tree, that is, using the wavelet transform of multiple iterations to analyze the input signal. The schematic diagram of WPD is shown in Figure 2. In Figure 2, from the left side to the right side, the signal components acquired by decomposing the original signal in 1st layer, 2nd layer, . . . , and m -th layer are represented, respectively; S represents the original signal, which is decomposed in m ($m \geq 1$) layers to acquire the corresponding low-frequency parts $S_{m,0}$ and high-frequency parts $S_{m,k}$.

Table 1. Maximum limits of wind farm output power variation of GB/T 19963-2011 standard [21].

Installation Capacity of Wind Farm (MW)	Maximum Power Variation in 1 Min (MW)	Maximum Power Variation in 10 Min (MW)
<30	3	10
30–150	Installation capacity / 10	Installation capacity / 3
>150	15	50

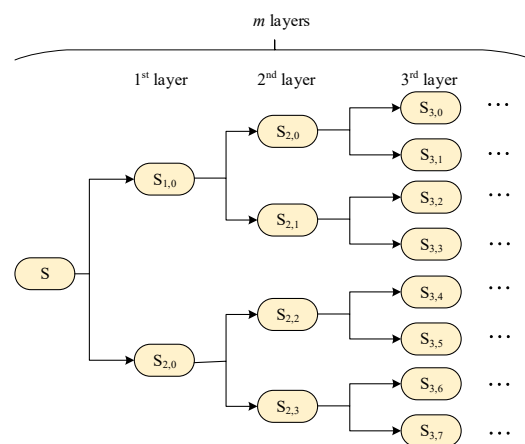


Figure 2. Schematic diagram of WPD.

The wavelet packet algorithm includes two processes: decomposition and reconstruction of wave packets. The expression of the WPD process is shown in (3).

$$\begin{cases} f_p^{j,2m} = \sum_{k=1}^m h_{k-2p} f_k^{j+1,m} \\ f_p^{j,2m+1} = \sum_{k=1}^m g_{k-2p} f_k^{j+1,m} \end{cases} \quad (3)$$

The expression of wavelet packet reconstruction process is shown in (4).

$$f_p^{j+1,2m} = \sum_{k=1}^m (h_{p-2k} f_k^{j,2m} + g_{p-2k} f_k^{j,2m+2}) \quad (4)$$

where $f_p^{j,2m}$, $f_p^{j,2m+1}$ are the WPD factors, respectively; h and g are the factors of the low-pass and high-pass filters for each decomposition and reconstruction.

dbN wavelet has strong local analysis ability in the frequency domain and ideal amplitude-frequency characteristics, so it is widely used in engineering practice. Therefore, a high-order db5 wavelet is used in this study to decompose the original wind power output signal S in m layers. The decomposed signal is divided into 2^m frequency band signals, and the bandwidth of each signal frequency band in the m -th layer is $\Delta f = \frac{f_s}{2^{m+1}}$. Since the number of decomposition layers in the traditional WPD method needs to be manually selected, which lacks objectivity, and the number of decomposition layers is often different under different wind power output scenarios. Therefore, in order to improve the general applicability of WPD in different wind farm capacities and different wind power fluctuation scenarios, adaptive WPD is adopted in this study; its decomposition process is as follows:

- (1) Let $m = 1$ and then decompose the original wind power;
- (2) Calculate whether the decomposed low-frequency part $S_{m,0}$ meets the standard in Table 1;
- (3) If the standard in Table 1 is not met, let $m = m + 1$, continue to decompose the original wind power and step (2) is repeated; If the standard in Table 1 is met, m is the best WPD layer, then let $P_{\text{grid}}(t) = S_{m,0}$. In this way, the grid-connected power is acquired. The difference between $P_{\text{grid}}(t)$ and $P_w(t)$ is the reference output power $P_{\text{href}}(t)$ of HESS.

The process diagram of wind power fluctuation suppression by the adaptive WPD method is shown in Figure 3. After the original wind power is decomposed by adaptive WPD, the low-frequency component $S_{m,0}$ satisfying the fluctuation standard in Table 1, is obtained as the grid-connected power, and the remaining high-frequency fluctuation components are suppressed by HESS.

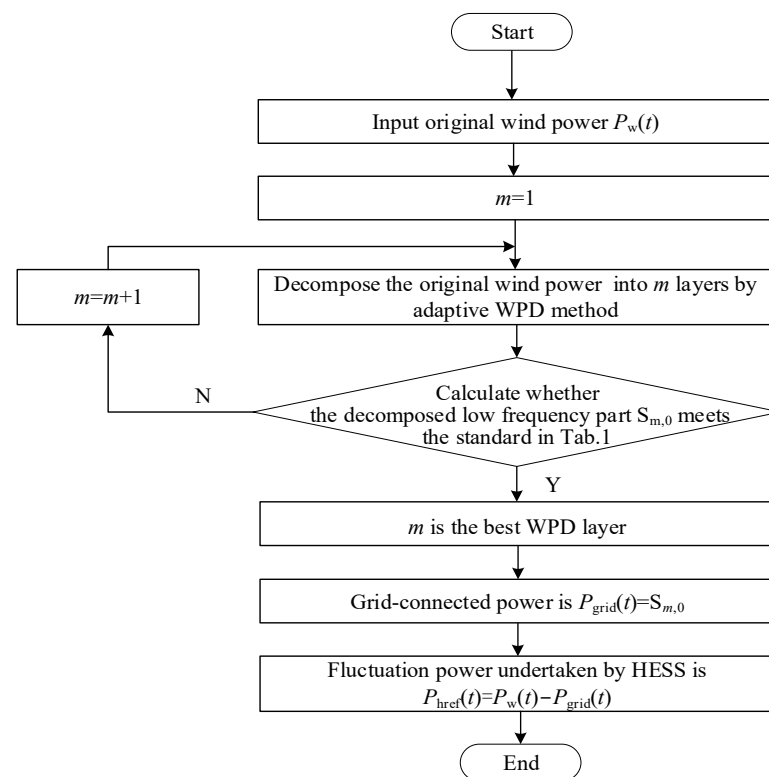


Figure 3. Process diagram of wind power fluctuation suppression by adaptive WPD method.

3. Initial Power Distribution and Charge–Discharge States Analysis of HESS

3.1. Initial Power Distribution of BESS Based on Adaptive WPD

According to the different technical characteristics of energy-type and power-type energy storage, how to rationally distribute the power of HESS is a key factor affecting the power suppression effect of wind power. Since the lifetime of the battery may be reduced if the charge–discharge frequency is too fast, the battery is suitable for undertaking low-frequency power fluctuation. At the same time, the response speed of the supercapacitor is fast, and it can undertake high-frequency power instructions, which is suitable for frequent charge–discharge conversion scenarios. The charge–discharge response time of the battery and supercapacitor ranges from minutes to hours and milliseconds to minutes, respectively. Therefore, 1 min is chosen as the boundary between the charge–discharge response time of the battery and supercapacitor, and it can be calculated that the corresponding dividing frequency is 1.67×10^{-2} Hz. Therefore, according to the results of adaptive WPD in Section 2.2, the fluctuation power to be undertaken by the battery and the supercapacitor, respectively, is shown in (5).

$$\begin{cases} P_{bref} = -(S_{m,1} + S_{m,2} + \dots + S_{m,k}) \\ P_{scref} = -(S_{m,k+1} + S_{m,k+2} + \dots + S_{m,2^m-1}) \end{cases} \quad (5)$$

where P_{bref} and P_{scref} are the initial distribution power of battery and supercapacitor, respectively; f_s is the sampling frequency of the initial wind power signal; m is the number of decomposition layers; $S_{m,1}, S_{m,2}, \dots, S_{m,k}$ are high-frequency signal parts after being decomposed by wavelet packet; k is the frequency division point of battery and supercapacitor power signals.

3.2. Charge–Discharge States Analysis of HESS Based on Adaptive WPD

Low-pass filtering, EMD, WPD and other filter decomposition methods essentially decompose the original signal through a series of filtering processes with different filtering coefficients and then obtain high and low-frequency signal components. Therefore, when the methods above are applied to the power distribution of HESS, high and low-frequency wind power fluctuations are usually allocated to power type and energy type energy storage, respectively, according to the response frequency of HESS, while the cooperation between energy type and power type energy storage is ignored, resulting in inconsistent charge–discharge states in the same time sequence. With a 100 MW wind farm, adaptive WPD is adopted to decompose the original daily wind output power, the grid-connected power and initial distribution power of HESS are acquired, and the problem of inconsistent charge–discharge states in HESS is further explained.

The original wind power and the grid-connected power are shown in Figure 4. The initial distribution power signals of HESS are shown in Figure 5. According to Sections 2.2 and 3.1, it can be calculated that the number of optimal decomposition layers is $m = 5$, and the frequency division point of the battery and supercapacitor power signal is $k = 3$. In Figure 4, after WPD, the maximum fluctuation power of 100 MW wind farm at 1 min time scale decreases from the original 15.03 MW to 5.34 MW, and the grid-connected power is acquired, which satisfies the fluctuation standard in Table 1. Compared with the original wind power, grid-connected power has an obvious suppression effect. In Figure 5, the supercapacitor undertakes the high-frequency power command with frequent fluctuations, while the power command of the battery changes with a lower frequency and the amplitude is large, the less charge–discharge conversion times are beneficial to extend the lifetime of the battery. The power distribution results are in line with the technical properties of the battery and supercapacitor. However, the initial power command of HESS acquired by adaptive WPD has the problem that the charge–discharge time sequence of each energy storage technology is inconsistent. For example, in Figure 5, when $t = 554$ min, the HESS output power is $P_{hess}(t) = -2.36$ MW, the supercapacitor output power is $P_{sc}(t) = 3.24$ MW, the battery output power is $P_b(t) = -5.6$ MW. Besides, $|P_b(t)| > |P_{hess}(t)|$,

$|P_{sc}(t)| > |P_{hess}(t)|$. Therefore, we can observe that the battery is charging while the supercapacitor is discharging at this time; Moreover, the energy absorbed and released by each energy storage technology is greater than HESS. Such inconsistent charge–discharge states in the same time sequence can easily make the SOC approach its upper and lower limits, resulting in a decrease in the overall operating efficiency of HESS.

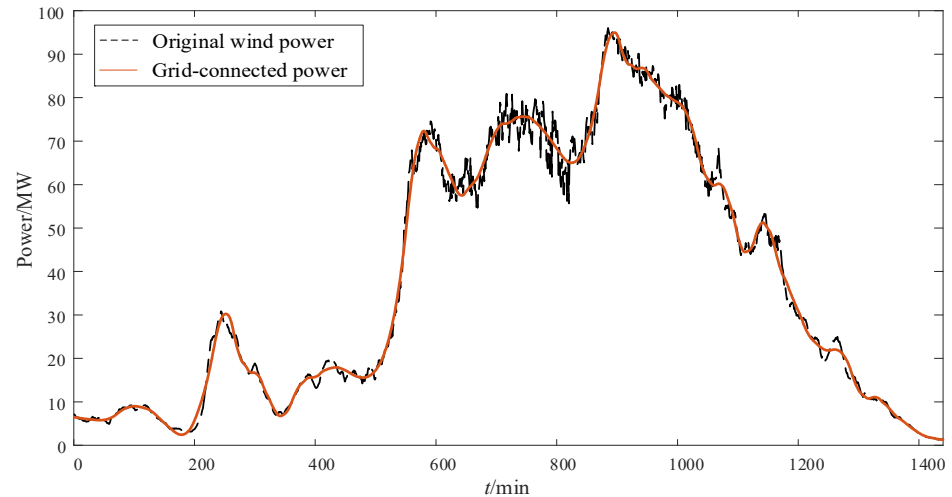


Figure 4. Original wind power and grid-connected power.

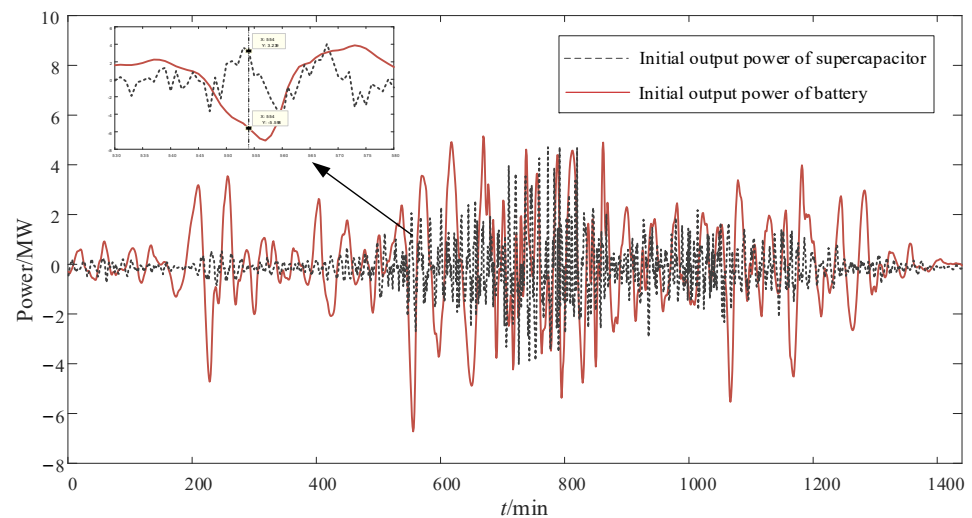


Figure 5. Initial distribution power of HESS.

4. HESS Fuzzy Optimal Control Considering Charge-Discharge Time Sequence

After the initial power distribution of HESS, the existing studies often optimize the SOC over-limit problem without considering the consistency of the charge–discharge time sequence. Therefore, before SOC optimization, a charge–discharge time sequence optimization method based on the consistency index is proposed to correct the initial power distribution of HESS for the first time. Then, aiming at the SOC over-limit problem, the fuzzy optimization method is adopted to correct the HESS output power for the second time; the charge–discharge optimization control strategy for the HESS is shown in Figure 6.

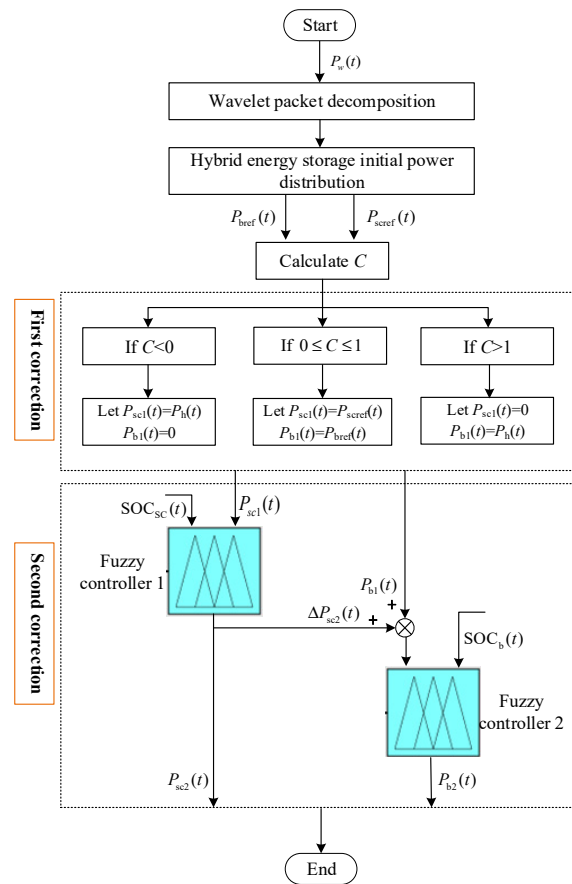


Figure 6. Charge–discharge optimization control strategy for HESS.

4.1. Charge–Discharge Time Sequence Optimization Based on Consistency Index

In order to judge the charge–discharge status of HESS, the charge–discharge consistency index C is defined, as shown in (6).

$$C = \frac{P_h(t) - P_{SC}(t)}{P_h(t)} \quad (6)$$

where $0 \leq C \leq 1$ means that both energy storage systems are in charge or discharge state, or that one kind of energy storage is in charge or discharge state and the other kind of energy storage doesn't work; $C < 0$ or $C > 1$ means that one kind of energy storage is in charge state while the other kind of energy storage is in discharge state.

Aiming at the problem of inconsistent charge–discharge states in the same sequence, a charge–discharge time sequence optimization is proposed to correct the initial power distribution of HESS for the first time. The optimization steps are as follows:

- (1) If $0 \leq C \leq 1$, keep the original charge–discharge strategies of the battery and supercapacitor unchanged.
- (2) If $C < 0$, that is, $|P_{sc}(t)| > |P_h(t)|$, which indicates that the HESS and supercapacitor are both in charge or discharge state, while the battery is in discharge or charge state, resulting in inconsistent charge–discharge states of different energy storage technologies in the same time sequence. In this case, let $P_{sc1}(t) = P_h(t)$, $P_{b1}(t) = 0$.
- (3) If $C > 1$, that is, $|P_{sc}(t)| < |P_h(t)|$, which indicates that the HESS and battery are both in charge or discharge state, while the supercapacitor is in discharge or charge state. In this case, let $P_{b1}(t) = P_h(t)$, $P_{sc1}(t) = 0$.

After the first correction, the battery and supercapacitor energy storage can synchronously suppress wind power fluctuation in the same time sequence.

4.2. Fuzzy Optimization of HESS Based on SOC

Traditional control theories require a clear mathematical model of the controlled object, which is generally used to solve the control problems of simple controlled systems, such as linearity and time invariance. Fuzzy control does not depend on the mathematical model of the controlled system but depends on the fuzzy rules converted from operating experience, and then converts these rules into computer language to realize automatic control, so it belongs to intelligent control. Due to the influence of the distributed inductance and distributed capacitance of the battery and supercapacitor energy storage, they are in a nonlinear state during the charge and discharge process. Therefore, the nonlinear degree of HESS composed of battery and supercapacitor is greatly increased. Fuzzy control is born to solve the nonlinear problem of the controlled object, so this study chooses the fuzzy algorithm to control the SOC of HESS. As shown in Figure 6, on the basis of the first correction, fuzzy optimization is adopted to correct the HESS output power for the second time to solve the SOC over-limit problem. Since the SOC of the battery and the supercapacitor may exceed the normal range during the actual operation of HESS, excessive charge and discharge will reduce the service life of the energy storage; two fuzzy controllers are selected to control the SOC of the battery and the supercapacitor, respectively. The first fuzzy controller takes $SOC_{SC}(t-1)$ and $\Delta SOC_{SC}(t)$ of the supercapacitor as two inputs, and the second fuzzy controller takes $SOC_b(t-1)$ and $\Delta SOC_b(t)$ of the battery as two inputs. The optimization steps are as follows:

- (1) Calculate the $SOC_{SC}(t)$ of the supercapacitor after the first correction; If $SOC_{SC}(t)$ is appropriate, keep the charge–discharge strategy of the supercapacitor after the first correction unchanged; If $SOC_{SC}(t-1)$ is too large and $\Delta SOC_{SC}(t) > 0$, or $SOC_{SC}(t-1)$ is too small and $\Delta SOC_{SC}(t) < 0$, it is necessary to make a second correction to the output power of supercapacitor. The output of the first fuzzy controller is the correction coefficient $K_{SC_SOC}(t)$. The supercapacitor power command after the second correction is $P_{sc2}(t) = K_{SC_SOC}(t) \cdot P_{sc1}(t)$. In order to obtain a good control effect, the following principles should be followed when designing the fuzzy control rules between input and output variables in the first fuzzy controller: when $\Delta SOC_{SC}(t) > 0$, the larger the $SOC_{SC}(t-1)$ and $\Delta SOC_{SC}(t)$, the smaller the output variable $K_{SC_SOC}(t)$; Similarly, when $\Delta SOC_{SC}(t) < 0$, the smaller the $SOC_{SC}(t-1)$ and $\Delta SOC_{SC}(t)$, the smaller the output variable $K_{SC_SOC}(t)$. $K_{SC_SOC}(t) \in [0, 1]$. So the membership functions and fuzzy rules for the first fuzzy controller are shown in Figure 7a and Table 3.
- (2) The difference between the power command of the supercapacitor before and after the second correction $\Delta P_{sc2}(t)$ is supplemented by the battery, that is, $\Delta P_{sc2}(t) = P_{sc1}(t) - P_{sc2}(t)$. The second fuzzy controller optimizes the $SOC_{b1}(t)$ of the battery based on the same strategy as step (1). The output of the second fuzzy controller is $K_{b_SOC}(t)$. The battery power command after second correction is $P_{b2}(t) = K_{b_SOC}(t) \cdot (P_{b1}(t) + \Delta P_{sc2}(t))$. The fuzzy design principles of the second fuzzy controller are the same as that of the first fuzzy controller. The membership functions and fuzzy rules for the second fuzzy controller are shown in Figure 7b and Table 2.

The difference between the HESS output power after two corrections and the initial HESS output power is $\Delta P_h(t)$. The system frequency is allowed to fluctuate in a small range during the operation of the power grid. The frequency fluctuation corresponds to the high-frequency unbalance power between the supply and demand side of the system; it can be absorbed by the frequency deviation accommodation capacity of the power grid. So $\Delta P_h(t)$ can be absorbed by the power grid itself. Therefore, after two corrections, the output power of HESS and the wind farm also conforms to the energy balance relationship in the wind storage system.

Table 2. Control rules for the second fuzzy controller.

$\Delta SOC_b(t)$	$SOC_b(t - 1)$						
	VQ	Q	PQ	H	PW	E	VE
SA	VQ	Q	PQ	H	PW	PW	VE
SD	VQ	PQ	PW	E	E	VE	VE
SF	VQ	PW	E	VE	VE	VE	VE
RD	VE	VE	VE	VE	VE	E	VQ
RF	VE	VE	VE	E	PW	PW	VQ
RA	VE	PW	PQ	PW	H	Q	VQ

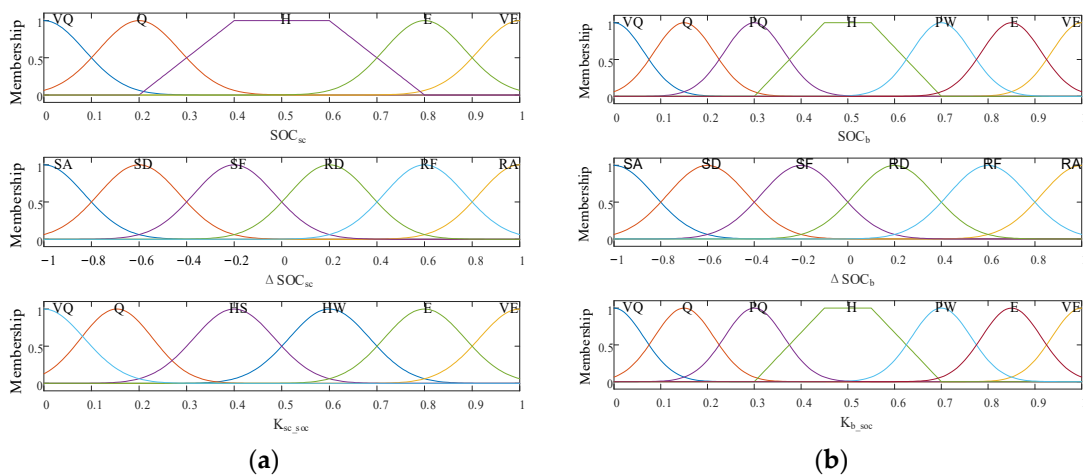


Figure 7. Membership functions for the two fuzzy controllers. (a) Membership functions of the first fuzzy controller; (b) Membership functions of the second fuzzy controller.

Table 3. Control rules for the first fuzzy controller.

$\Delta SOC_{SC}(t)$	$SOC_{SC}(t - 1)$				
	VQ	Q	H	E	VE
SA	VQ	Q	HS	HW	VE
SD	VQ	HW	E	VE	VE
SF	VQ	E	VE	VE	VE
RD	VE	VE	VE	E	VQ
RF	VE	VE	HW	HW	VQ
RA	VE	HW	HS	Q	VQ

According to the membership functions and fuzzy rules of the two fuzzy controllers, the relationship curves of input and output variables in the two fuzzy controllers are shown in Figure 8a,b, respectively. As seen in Figure 8, the two three-dimensional surfaces are basically smooth, and the relations between input and output variables meet the requirements of SOC correction of HESS, which indicate that the establishment of fuzzy control rules is basically qualified.

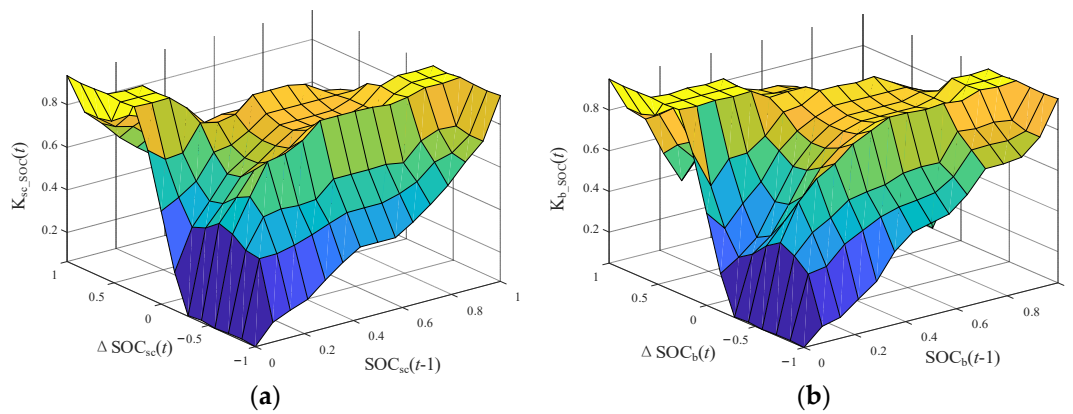


Figure 8. Relationship curves of input and output variables in the two fuzzy controllers. (a) Relationship curves of input and output variables in the first fuzzy controller; (b) Relationship curves of input and output variables in the second fuzzy controller.

5. Case Study

To verify the superiority of the proposed strategy, the typical daily output data of a 100 MW wind farm is adopted as the original wind power, whose fluctuation power can be suppressed by HESS. The structure of the wind storage system is the same as the one in Figure 1. The grid-connected power and the power optimization results of HESS are acquired by the optimization control strategy proposed in Section 4. The superiority of the proposed method is analyzed as follows from three aspects: suppression effect, charge–discharge time sequence optimization effect and SOC optimization effect.

5.1. Analysis of Suppression Effect of Wind Power Fluctuation

Figure 9 shows the original wind power and grid-connected power. The sampling time of original wind power is 1 min. After the original wind power is decomposed by the adaptive WPD method, we can calculate that the number of WPD layers is 6, and the frequency division point of the power signals of the battery and supercapacitor is $k = 4$. As seen from Figure 9, after WPD, the maximum power fluctuation at a 1 min time scale is reduced from 12.04 MW to 4.83 MW, so the grid-connected power meets the standard in Table 1. With the calculation method in [20], it can be obtained that the HESS suppresses 67.8% of the wind power fluctuation, so the grid-connected power has an obvious smoothing effect.

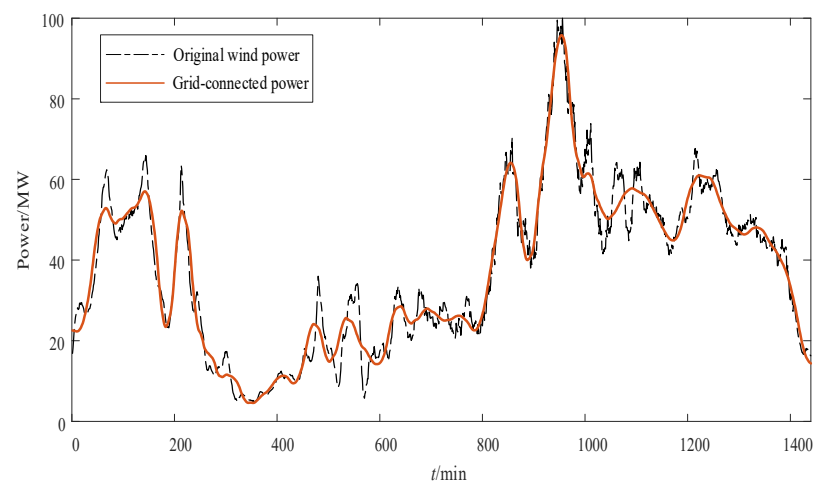


Figure 9. Original wind power and grid-connected power.

In order to demonstrate the general applicability of adaptive WPD in different wind power application scenarios, the typical daily output data of 25 MW, 60 MW and 100 MW wind farms are selected for analysis. Table 4 shows the wind power suppression effect under different wind farm capacities obtained by adaptive WPD. As seen from Table 4, the smaller the wind farm capacity, the smaller the fluctuation amplitude. According to the different power fluctuation characteristics in the wind farms with different capacities, the number of wavelet packet decomposition layers also changes accordingly, and the grid-connected power meets the fluctuation standard in Table 1 is finally obtained. Results in Table 4 show that the adaptive WPD can select the best WPD layer according to different wind power output scenarios, and the adaptive wind power decomposition can also be realized.

Table 4. Wind power suppression effect under different wind farm capacities based on adaptive WPD.

Capacity of Wind Farm (MW)	Maximum Power Variation in 1 Min in the Original Wind Power Signal (MW)	Maximum Power Variation in 1 Min in the Grid-Connected Power Signal (MW)	Number of Decomposition Layers
25	3.63	1.59	3
60	7.06	3.48	5
100	12.04	4.83	6

5.2. Analysis of Charge–Discharge Time Sequence Optimization of HESS

After the initial power distribution of HESS, aiming at the problem of inconsistent charge–discharge states, a charge–discharge time sequence optimization method is proposed to correct the initial power distribution for the first time. In order to compare the charge–discharge performance of the battery and supercapacitor before and after the first correction, Figures 10 and 11, respectively, show the initial output power of the HESS (without considering the charge–discharge time sequence optimization) and the output power after the first correction (considering the charge–discharge time sequence optimization). In Figure 10, during the period of 320 min–445 min, without optimizing the charge–discharge time sequence, the encircled parts indicate that the charge–discharge states of the battery and supercapacitor are inconsistent, resulting in additional energy absorption and release. In Figure 11, the battery and supercapacitor can be controlled to charge or discharge synchronously in the same time sequence after the first correction. Compared with the unoptimized results in Figure 10, the charge–discharge conversion times of the battery obtained by the first correction in Figure 11 are reduced from 71 to 14 times, and the charge–discharge conversion times of the supercapacitor in Figure 11 are reduced from 390 to 61 times; The cumulative reduction of unnecessary charge–discharge energy is 12.12 MWh. Therefore, after the first correction, the charge–discharge conversion times and the accumulated charge–discharge energy are greatly reduced, which is beneficial for improving the service life of HESS.

5.3. Analysis of SOC Optimization Effect of HESS

According to the calculation method in [22], the capacities of the battery and supercapacitor are 5.98 MWh and 1.69 MWh, respectively. In order to illustrate the effectiveness of the method proposed in this study, the lower and upper limits of SOC are set to 0.2 and 0.8, respectively, and two control methods are used to optimize the SOC of HESS, which are: ① The fuzzy control method in literature [22]; ② The fuzzy control method considering charge–discharge time sequence proposed in this study. The SOC curves of the battery and supercapacitor under different control strategies are shown in Figures 12 and 13. As seen from Figures 12 and 13, both control methods can control the SOC of the battery and supercapacitor between [0.2, 0.8]. The SOC curves of battery energy storage under the two control methods are similar, while the SOC curves of supercapacitor energy storage under the two control methods vary greatly with time. Although the first control method can control the SOC of the supercapacitor between [0.2, 0.8], the SOC changes frequently and

greatly, and the supercapacitor is in a high charge–discharge margin for nearly 30% of the time. Compared with the first control method, the working range of the supercapacitor SOC obtained by the fuzzy control method proposed in this study is greatly improved. The SOC curve is relatively flat, and the SOC is maintained between [0.4, 0.6] for about 90% of the time. Therefore, the fuzzy control method considering the charge–discharge time sequence proposed in this study can effectively reduce the charge–discharge depth of the energy storage system and prevent excessive charge–discharge. After two corrections of HESS output power by using the charge–discharge time sequence optimization method and fuzzy optimization method, the final output power of HESS is shown in Figure 14.

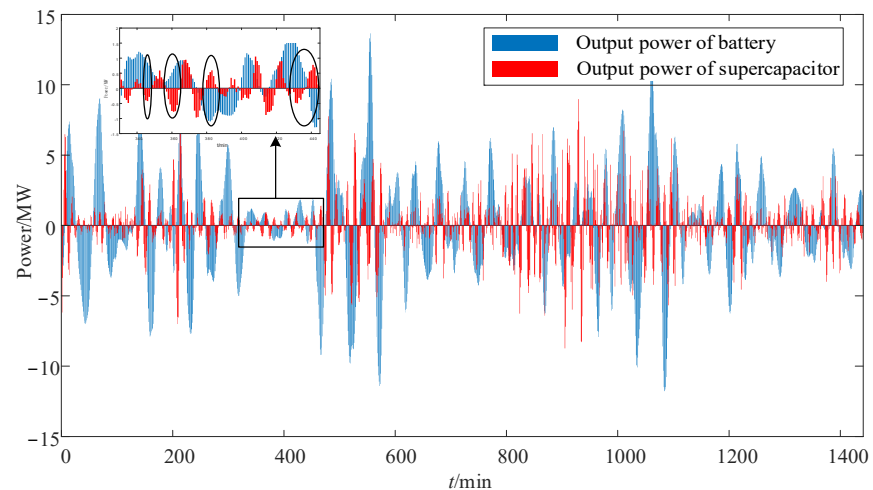


Figure 10. The initial output power of HESS (not considering charge–discharge time sequence optimization).

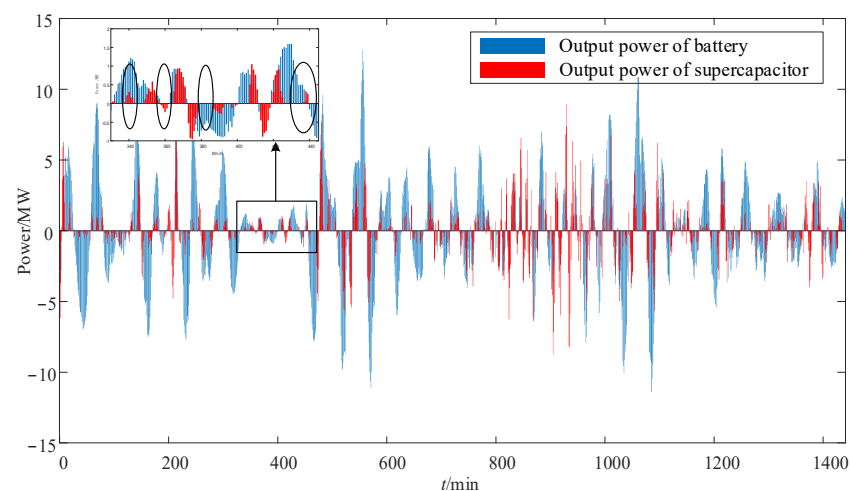


Figure 11. The output power of HESS after the first correction (considering charge–discharge time sequence optimization).

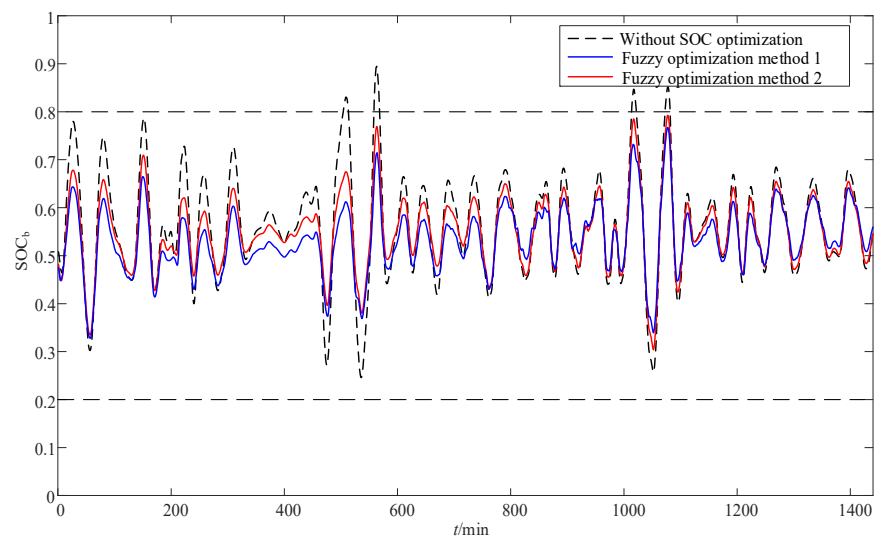


Figure 12. SOC curves of battery before and after correction.

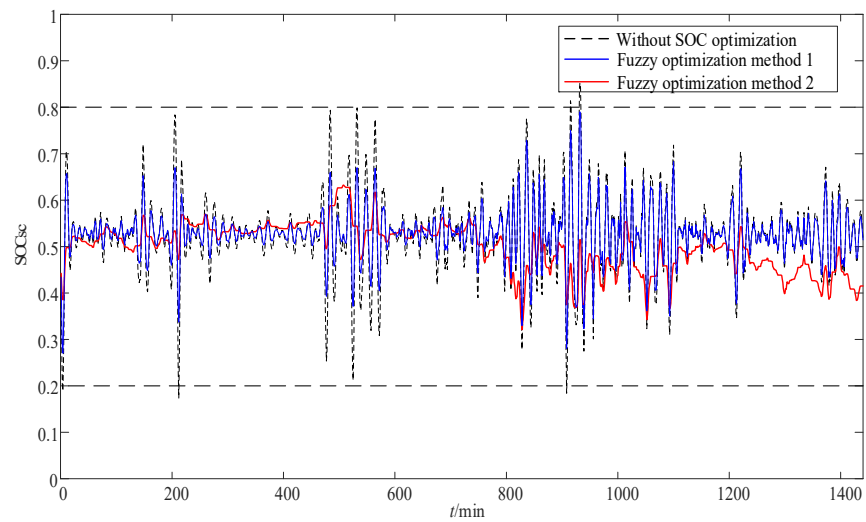


Figure 13. SOC curves of supercapacitor before and after correction.

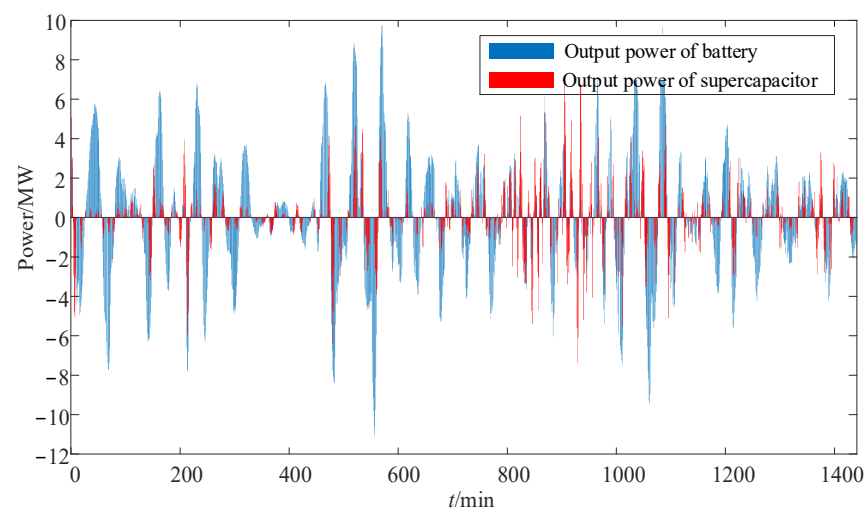


Figure 14. The final output power of HESS after two corrections.

5.4. Sensitivity Analysis of Different Frequency Division Points on Optimization Results

In order to analyze the influence of different frequency division points on the optimization results of HESS, 1 min, 2 min, and 3 min are chosen as the boundary of response time between the battery and supercapacitor, respectively. After the original wind output power is decomposed by adaptive WPD, the frequency range of each signal component is shown in Table 5. According to the frequency range of each signal, it can be determined that the corresponding frequency division points under the boundary response time of 1 min, 2 min and 3 min are $k = 4$, $k = 2$, and $k = 1$, respectively. The optimization results under three frequency division points are shown in Table 6. As seen from Table 6, when the boundary response time increases, the cases of inconsistent charge–discharge states in HESS increase, so the cumulative reduction of unnecessary charge–discharge energy after the first correction also increases. We can also observe that increasing the boundary response time can reduce the charge–discharge conversion times of the battery but increase the charge–discharge conversion times of the supercapacitor. With the change in the boundary response time, the changes in the charge–discharge conversion times and charge–discharge energy reduction of the battery are not obvious, which indicates that the optimization results of the battery are not sensitive to the small range change of boundary response time. Besides, no matter how the boundary response time is selected, the charge–discharge conversion times of the battery and supercapacitor are significantly reduced after the first correction, which indicates that the charge–discharge time sequence optimization method proposed in this study can obtain good results under different frequency division points.

Table 5. The frequency range of each signal component after adaptive WPD.

Signal Component after Adaptive WPD	Frequency Range (Hz)
$S_{m,1}$	3.91×10^{-3} – 5.86×10^{-3}
$S_{m,2}$	5.86×10^{-3} – 7.81×10^{-3}
$S_{m,3}$	7.81×10^{-3} – 1.17×10^{-2}
$S_{m,4}$	1.17×10^{-2} – 1.56×10^{-2}
$S_{m,5}$	1.56×10^{-2} – 1.95×10^{-2}
$S_{m,6}$	1.95×10^{-2} – 2.34×10^{-2}
...	...

Table 6. Optimization results under different frequency division points.

Response Time Boundary of HESS (Min)	Dividing Frequency of HESS (Hz)	Frequency Division Point of HESS	Proportion of Inconsistent Charge–Discharge States before Correction	Charge–Discharge Conversion Times of Battery before and after Correction	Charge–Discharge Conversion Times of Supercapacitor before and after Correction	Charge–Discharge Energy Reduction after Correction (MWh)
1	1.67×10^{-2}	$k = 4$	49.8%	71, 14	390, 61	12.12
2	8.33×10^{-3}	$k = 2$	50.1%	69, 10	425, 69	13.11
3	5.56×10^{-3}	$k = 1$	52.4%	61, 8	464, 75	13.90

Since the response time of the energy storage system is related to its type and capacity, when the adaptive WPD is used to distribute the power of HESS, the selection of frequency division point of energy-type and power-type energy storage may affect the optimization results. The larger the wind farm capacity is, the greater the wind power fluctuation tends to be. In this case, the influence of frequency division point selection on the optimization results in HESS will also become larger. Therefore, in the scenario of large wind farm capacity, sensitivity analysis of different frequency division points can be carried out, combined with the actual type and capacity of the energy storage system, to select the appropriate frequency division point.

6. Conclusions

In this study, the battery-supercapacitor HESS is established to suppress the wind power fluctuation and the wavelet packet-fuzzy optimization control strategy considering charge–discharge time sequence is proposed to optimize the output power of the HESS. The superiority of the proposed method is verified and analyzed with a 100 MW wind farm from three aspects: suppression effect, charge–discharge time sequence optimization effect and SOC optimization effect. The main conclusions are as follows:

- (1) By comprehensively analyzing the properties of wind power fluctuation and HESS, the grid-connected power that meets the GB/T 19963-2011 standard is obtained, and the initial power distribution of HESS is realized by the adaptive WPD method; The adaptive WPD method has a good suppression effect on the original wind power fluctuation, and it can be applied to different wind power fluctuation scenarios.
- (2) The proposed power optimization distribution method for HESS considering charge–discharge time sequence can enable the battery and supercapacitor to charge or discharge synchronously in the same time sequence, thus greatly reducing the charge–discharge conversion times and accumulated charge–discharge energy. Moreover, the fuzzy control method considering the charge–discharge time sequence proposed in this study can effectively reduce the charge–discharge depth of the energy storage system and prevent excessive charge–discharge, which is conducive to improving the lifetime and economy of the HESS.

Overall, this study presents a comprehensive approach that combines adaptive wavelet packet decomposition, charge–discharge time sequence optimization, and fuzzy optimization methods to address the challenges associated with HESS power distribution strategies, with the potential to improve the efficiency and performance of wind farms and HESS. The proposed approach can solve the problem of inconsistent charge–discharge states of energy-type and power-type energy storage and achieve optimal operation of HESS. Therefore, it is of great significance for the sustainable development of energy storage systems and the electricity power industry.

Author Contributions: Methodology, X.Z. and Y.Z. (Yunxiao Zhang); Validation, X.Z. and X.C.; Data analysis, E.S. and X.Z.; Writing—original draft preparation, X.Z., J.Q. and L.W.; Writing—review and editing, Y.Z. (Yongchang Zhang) and H.Z.; Supervision, Y.Z. (Yongchang Zhang) and H.Z. All authors have read and agreed to the published version of the manuscript.

Funding: This research was funded by the National Key R&D Program of China (Grant No. 2021YFB2400702).

Institutional Review Board Statement: Not applicable.

Informed Consent Statement: Not applicable.

Data Availability Statement: Not applicable.

Conflicts of Interest: Author Erfa Shang is employed by Inner Mongolia Xilin Gol League Dian Tou New Energy Co., Ltd. The remaining authors declare that the research was conducted in the absence of any commercial or financial relationships that could be construed as a potential conflict of interest.

References

1. Sun, Y.; Tang, X.; Sun, X.; Jia, D.; Cao, Z.; Pan, J.; Xu, B. Model predictive control and improved low-pass filtering strategies based on wind power fluctuation mitigation. *J. Mod. Power Syst. Clean Energy* **2019**, *7*, 512–524. [[CrossRef](#)]
2. Xie, H.; Jiang, M.; Zhang, D.; Goh, H.H.; Ahmad, T.; Liu, H.; Liu, T.; Wang, S.; Wu, T. IntelliSense technology in the new power systems. *Renew. Sustain. Energy Rev.* **2023**, *177*, 113229. [[CrossRef](#)]
3. Zhang, D.; Zhu, H.; Zhang, H.; Goh, H.H.; Liu, H.; Wu, T. Multi-Objective Optimization for Smart Integrated Energy System Considering Demand Responses and Dynamic Prices. *IEEE Trans. Smart Grid* **2022**, *13*, 1100–1112. [[CrossRef](#)]
4. Nadeem, F.; Hussain, S.M.S.; Tiwari, P.K.; Goswami, A.K.; Ustun, T.S. Comparative review of energy storage systems, their roles, and impacts on future power systems. *IEEE Access* **2019**, *7*, 4555–4585. [[CrossRef](#)]
5. Meng, L.; Zafar, J.; Khadem, S.K.; Collinson, A.; Murchie, K.C.; Coffele, F.; Burt, G.M. Fast frequency response from energy storage systems—a review of grid standards, projects and technical Issues. *IEEE Trans. Smart Grid.* **2019**, *11*, 1566–1581. [[CrossRef](#)]

6. Ren, Y.; Xue, Y.; Yun, P. Multi-objective optimal energy storage system for reducing power fluctuation of wind farm via markov prediction. *Power Syst. Autom.* **2020**, *44*, 67–74. (In Chinese)
7. Barelli, L.; Ciupageanu, D.-A.; Ottaviano, A.; Pelosi, D.; Lazaroiu, G. Stochastic power management strategy for hybrid energy storage systems to enhance large scale wind energy integration. *J. Energy Storage* **2020**, *31*, 101650. [[CrossRef](#)]
8. Qais, M.H.; Hasanien, H.M.; Alghuwainem, S. Output power smoothing of wind power plants using self-tuned controlled SMES units. *Electr. Power Syst. Res.* **2020**, *178*, 106056. [[CrossRef](#)]
9. Shi, J.; Wang, L.; Lee, W.-J.; Cheng, X.; Zong, X. Hybrid Energy Storage System (HESS) optimization enabling very short-term wind power generation scheduling based on output feature extraction. *Appl. Energy* **2019**, *256*, 113915. [[CrossRef](#)]
10. Zou, J.; Dai, B.; Peng, C.; Xin, X.; Luo, W. Wind power smoothing method using hybrid energy storage system based on SOC hierarchical optimization. *Power Syst. Autom.* **2013**, *37*, 1–6. (In Chinese)
11. Sun, Y.; Tang, X.; Sun, X.; Jia, D.; Wang, P.; Zhang, G. Research on multi-type energy storage coordination control strategy based on MPC-HHT. *Proc. CSEE* **2018**, *38*, 2580–2588. (In Chinese)
12. Rasool, S.; Muttaqi, K.M.; Sutanto, D. A multi-filter based dynamic power sharing control for a hybrid energy storage system integrated to a wave energy converter for output power smoothing. *IEEE Trans. Sustain. Energy* **2022**, *13*, 1693–1706. [[CrossRef](#)]
13. Zhang, Q.; Li, X.; Yang, M.; Cao, Y.; Li, P. Capacity determination of hybrid energy storage system for smoothing wind power fluctuations with maximum net benefit. *Trans. China Electrotech. Soc.* **2016**, *31*, 40–48. (In Chinese)
14. Han, X.; Tian, C.; Cheng, C. Power allocation method of hybrid energy storage system based on empirical mode decomposition. *Acta Energ. Sol. Sinca* **2014**, *35*, 1889–1896.
15. Jiang, Q.; Hong, H. Wavelet-Based Capacity Configuration and Coordinated Control of Hybrid Energy Storage System for Smoothing Out Wind Power Fluctuations. *IEEE Trans. Power Syst.* **2013**, *28*, 1363–1372. [[CrossRef](#)]
16. Trung, T.T.; Ahn, S.-J.; Choi, J.-H.; Go, S.-I.; Nam, S.-R. Real-Time Wavelet-Based Coordinated Control of Hybrid Energy Storage Systems for Denoising and Flattening Wind Power Output. *Energies* **2014**, *7*, 6620–6644. [[CrossRef](#)]
17. Wu, J.; Ding, M. Wind power fluctuation smoothing strategy of hybrid energy storage system using self-adaptive wavelet packet decomposition. *Power Syst. Autom.* **2017**, *41*, 7–12. (In Chinese)
18. Krim, Y.; Abbes, D.; Krim, S. Control and fuzzy logic supervision of a wind power system with battery/supercapacitor hybrid energy storage. In Proceedings of the 2018 7th International Conference on Systems and Control (ICSC), Valencia, Spain, 24–26 October 2018; pp. 180–187.
19. Cohen, I.J.; Wetz, D.A.; McRee, B.J.; Dong, Q.; Heinzl, J.M. Fuzzy logic control of a hybrid energy storage module for use as a high rate prime power supply. *IEEE Trans. Dielectr. Electr. Insul.* **2017**, *24*, 3887–3893. [[CrossRef](#)]
20. Miao, F.; Tang, X.; Qi, Z. Fluctuation feature extraction of wind power. In Proceedings of the IEEE PES Innovative Smart Grid Technologies, Tianjin, China, 21–24 May 2012; pp. 1–5.
21. GB/T 19963-2011; Technical Rule for Connecting Wind Farm to Power System. China Quality and Standards Publishing & Media Co., Ltd.: Beijing, China, 2011.
22. Jia, W.; Ren, Y.; Xue, Y. Wavelet packet-fuzzy control of hybrid energy storage for power fluctuation smoothing of large wind farm. *Acta Energ. Sol. Sin.* **2021**, *42*, 357–363.

Disclaimer/Publisher’s Note: The statements, opinions and data contained in all publications are solely those of the individual author(s) and contributor(s) and not of MDPI and/or the editor(s). MDPI and/or the editor(s) disclaim responsibility for any injury to people or property resulting from any ideas, methods, instructions or products referred to in the content.